

Neuron, Volume 69

Supplemental Information

## Neuronal Dynamics Underlying High- and Low-Frequency EEG Oscillations Contribute

### Independently to the Human BOLD Signal

René Scheeringa, Pascal Fries, Karl-Magnus Petersson, Robert Oostenveld, Iris Grothe, David G. Norris, Peter Hagoort, and Marcel C.M. Bastiaansen

## Supplemental Experimental Procedures

### Experimental Paradigm

It has been established that neuronal synchronization in the gamma frequency range is associated, amongst others, with attentional processes, most notably in the visual system (Bichot et al., 2005; Fries et al., 2001; Lakatos et al., 2008). Therefore, subjects engaged in a visual attention task that is known to elicit strong, long-lasting (up to several seconds), and narrow-band gamma activity in the MEG (Hoogenboom et al., 2006). In this task, subjects attend to circular, inward moving gratings, and are asked to detect a change in inward speed.

Each trial started with a reduction in contrast of a fixation point that was present between trials (Gaussian of  $0.4^\circ$ ) by 40%. This contrast reduction served as a warning for the upcoming visual stimulation, and instructed the subjects to stop blinking until the end of the trial. After 1100 ms, the fixation point was replaced by a sine wave grating (diameter:  $7^\circ$ ; spatial frequency: 2.5 cycles/degree; contrast: 100%). The sine wave grating contracted to the fixation point (1.6 degrees/sec) for one of four stimulus durations: 700, 1050, 1400 or 1750 ms. This was followed by an increase of the contraction speed to 2.2 degrees/sec for maximally 500 ms. Each stimulation length occurred in 20% of the trials. The remaining 20% percent of trials were catch trials without a speed change. Here the stimulus duration was 2100 ms.

Subjects were instructed to press a button with their right index finger as soon as they detected the speed change. The stimulus disappeared after a response was given, after 2100 ms of stimulation (for catch trials), or if no response was given within 500 ms after the speed change. Feedback about the performance was given for 500 ms. In the case of a correct response or if a response was correctly withheld, 'ok!' appeared in green above the fixation point. In case of

premature or slow/no responses, ‘early’ or ‘late’ respectively appeared in red. Trials were triggered by the onset of an fMRI volume, and occurred every two volumes. FMRI images were recorded in 330 ms, followed by a 3300 ms scan free period. This scan-free period allowed us to collect EEG data that were free of gradient artifacts during the visual stimulation interval.

In total, four blocks of 100 trials (20 of each trial length) were administered. One block had a length of approximately 12.30 minutes. All trials were projected on a screen at the back of the MRI scanner, which was made visible for subjects via a mirror mounted on the head coil. All stimuli were presented using the ‘Presentation’ software package (Neurobehavioral Systems, Inc.).

The relatively fast and regular pace of the task (in terms of fMRI design) may lead to BOLD-response overlap. The trials are however spaced more than 5 seconds apart, which is long enough to assume that the responses add up linearly and can therefore be adequately modeled in the context of the general linear model. The overlap does have as a consequence that the task related variance in the BOLD signal is smaller compared to a paradigm with wider spaced jittered trial presentation, which reduces the statistical power to detect task induced changes here. For trial-by-trial fluctuations in power it is not possible to a priori predict the effect of the temporal spacing of the trials has on the ability to detect a relation with the BOLD signal, since the time-scale at which these fluctuations around the mean response occur is unknown in advance. The results however indicate that in both cases there is sufficient statistical power to demonstrate a significant relation with the BOLD signal.

### **MRI Data Acquisition**

MRI data were acquired using a 3.0-T whole body MRI scanner (Siemens Magnetom Trio Tim, Siemens, Erlangen, Germany). A custom built eight channel array (Stark Contrast, MRI Coils,

Erlangen, Germany; Barth and Norris, 2007), covering the occipital cortex was used to record the functional images. Eight slices positioned parallel to the calcarine sulcus were recorded using a gradient echo EPI sequence (TE=30 ms, 90° flip angle, 4.0 mm slice thickness, 0.4 mm gap, voxel size 3.5 by 3.5 by 4.0 mm, bias field correction filter was turned on). In order to speed up image acquisition, no fat suppression was used, and a GRAPPA parallel imaging sequence was used with an acceleration factor of 2. As a result, one volume was registered in 330 ms. Each volume was followed by a 3300 ms gap (for gradient-free EEG recording). This resulted in a TR of 3630 ms. As a result of these parameters, the (theoretical) peak of the BOLD signal resulting from a given trial was reached approximately two TR's after the onset of that trial (see figure 1).

An anatomical MR was acquired with the same head coil and slice position as the EPI data. A 3D MPRAGE sequence was used (TE=3.49 ms, TR= 2300 ms, 10° flip angle, 80 slices per slab, 1mm slice thickness, 0.5 mm gap, GRAPPA acceleration factor=2, FOV=224 mm, voxel size 0.9 by 0.9 by 1.0 mm, bias field correction filter was turned on).

### **EEG Data Acquisition**

EEG data was recorded with a custom made MRI compatible cap equipped with carbon wired Ag/AgCL electrodes (Easycap, Herrsching-Breitbrunn, Germany). Data were recorded from 29 scalp sites selected from the 128 channel international 10-10 system (Fp1, Fp2, F3, F4, C3, C4, P3, P4, O1, O2, F7, F8, T7, T8, P7, P8, Fz, Pz, TP9, TP10, PO3, PO4, O9, O10, PO7, PO8, POz, Oz, Iz). The placement of the electrodes was focused over posterior regions, so that signals coming from visual regions could be recorded with greater accuracy. Two dedicated electrodes were placed on the sternum and clavicle to record the ECG. One additional electrode was placed under the right eye to record eye movements. The reference electrode was placed at Cz. A 250 Hz low-pass analogue hardware filter was placed between the electrode cap and the MRI

compatible EEG amplifier (BrainAmp MR plus, Brainproducts, Munich, Germany). The EEG was recorded with a 10-second time constant and continuously sampled at 5 kHz. EEG recordings were performed with Brain Vision Recorder software (Brainproducts GmbH, Germany).

### **FMRI Data Analysis**

FMRI data of each subject was corrected for movements, coregistered to the individual anatomical scan and smoothed with a 6 mm FWHM isotropic Gaussian kernel in SPM5 (Wellcome Department of Imaging Neuroscience, London, UK; see <http://www.fil.ion.ucl.ac.uk/spm>). In SPM5, a GLM was constructed to isolate the voxels that showed activation related to the visual stimulation. For each block, the visual stimulation was modelled by a regressor that was formed by convolving mini-blocks of the length of the visual stimulation period up until the speed change with the canonical HRF as implemented in SPM5. In addition to this regressor, the design matrix contained a regressor that modelled the behaviourally erroneous trials and a regressor for each of the six movement parameters. Significance was assessed by testing whether the beta values of the regressor modeling the visual stimulation period was larger than zero in a t-contrast. For each single subject, all voxels with a t-value greater than 10 formed a region of interest for the integrated EEG-fMRI analysis (see the right-hand panels of supporting figure S1 for the resulting BOLD activation maps for each single subject).

### **EEG Data: Preprocessing**

Preprocessing of the EEG data was carried out in Vision Analyzer (Brainproducts GmbH, Germany). The recorded EEG was first down sampled to 1000 Hz, and rereferenced to common

average. The original reference electrode was recomputed as electrode Cz. Subsequently, the data was segmented in epochs that started 750 ms before onset of visual stimulation, and ended either 400 ms after the speed change, or 400 ms after the end of stimulation in the catch trials. These segments were visually checked for artifacts, and trials with anomalies such as eye blinks and large muscle artifacts were removed. Behaviourally erroneous trials were excluded from further analysis.

### **EEG Data: ICA-Based Denoising**

To denoise the data, we used a two-step independent component analysis (ICA) approach adapted from a similar approach applied by Debener et al. (2005). Each ICA step was performed with the extended infomax algorithm (Lee et al., 1999) as implemented in EEGLab 5.03, (Delorme and Makeig, 2004), using a weight change of  $10^{-7}$  as a stop criterion.

In a first step, ICA was performed on the 45-100 Hz band-pass filtered EEG data. The unmixing matrix thus obtained was applied on the unfiltered data. The resulting component time courses therefore have a broadband spectral content, and were subsequently subjected to a time-frequency analysis as described in the previous section.

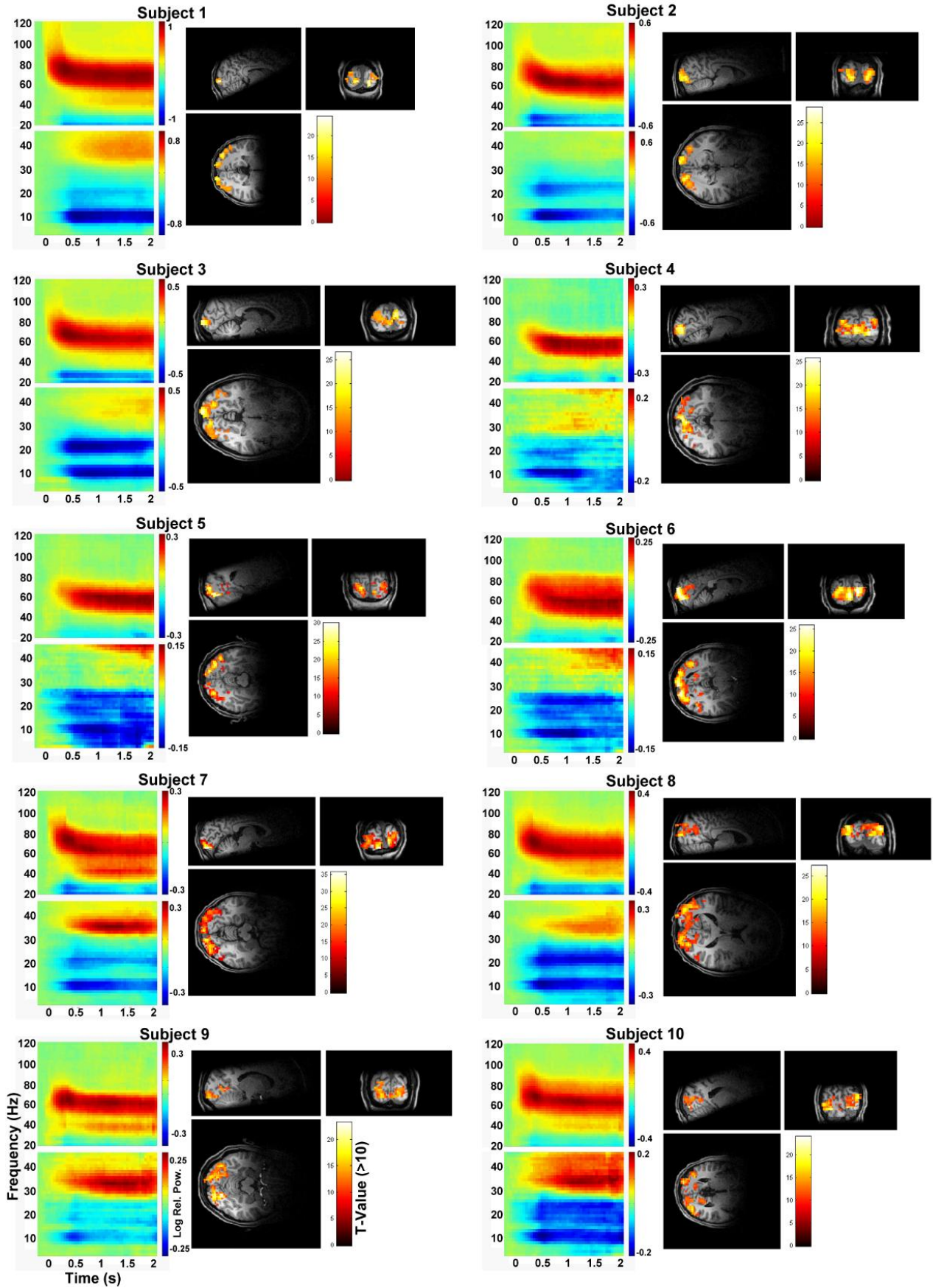
For all subjects, we were now able to observe a sustained gamma band response in some of the independent component time courses, with some inter-individual variation in the peak frequency of this response. In a second step, we again applied ICA, but this time on EEG data that was band-pass filtered with a narrow band of 10-20 Hz (depending on the spectral extent of each subject's gamma response) around the individually adjusted peak of the sustained gamma response). The unmixing weights of this analysis were again applied on the unfiltered data, and a time-frequency analysis was run on the component time courses.

Components that showed a sustained gamma band response were selected (1-5 components for

each subject) and projected back to channel level. Finally, these channel-level data were again subjected to a time-frequency analysis, separately for the lower and the higher frequency windows, as described in the previous section. The results of this analysis constitute the basis for the construction of regressors that were used in the integrated EEG fMRI analysis.

This strategy proved to be the best strategy to denoise the EEG data across the different frequency bands that have been reported before (Hoogenboom et al., 2006; Koch et al., 2009). For comparison, this ICA denoising strategy analysis was repeated for 30Hz low-pass filtered data. After applying the unmixing weights on unfiltered data many components showed a power decrease in alpha and beta bands, but only a few components also showed a sustained band limited gamma band effect. Only components that showed this gamma effect were selected and projected back to channel level. Although similar effects are observed in the alpha and beta bands, this strategy however proved to be inadequate to optimally denoise the EEG in the gamma band. The relative increase to baseline was lower, indicating more residual gamma band noise, resulting in the lack of gamma-BOLD coupling. The results of this analysis are presented in Supplemental Figures S2.

# Individual EEG & FMRI effects: Subjects 1-10





# Individual EEG & fMRI effects: Subjects 11-20

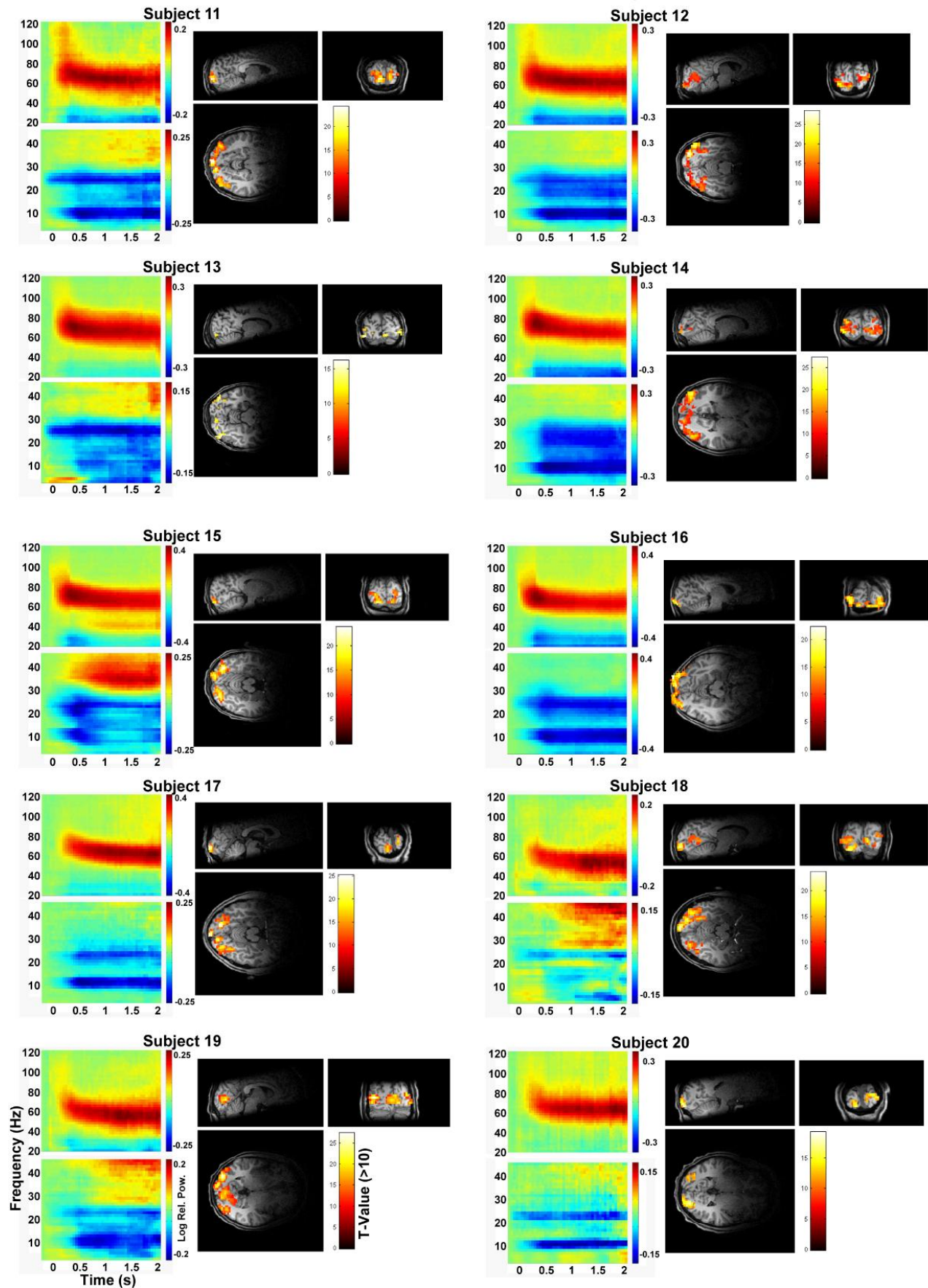


Figure S1, Related to Figure 2. Individual, ICA-Denoised Time-Frequency Analysis of the EEG, and BOLD Activations for All Subjects

ICA unmixing weights were estimated on individual gamma band filtered EEG data. The time-frequency analysis is the average across the channels selected for regressor construction. Separate time-frequency representations are depicted for low (2.5-45 Hz) and high (10-120 Hz) frequency windows, using different frequency smoothing. The values represent the log-transformed power values relative to baseline. T-maps ( $t > 10$ ) of the individual fMRI activations induced by visual stimulation are shown for each subject.

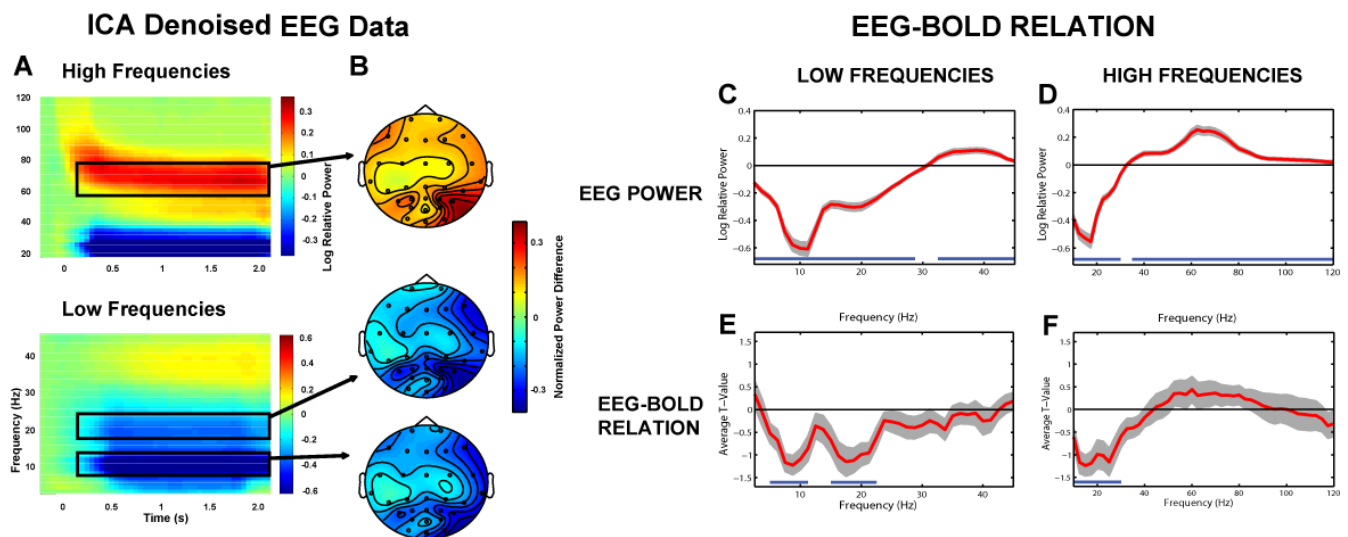


Figure S2, Related to Figures 2 and 3. Results for EEG after ICA Denoising with Unmixing Weights Estimated on EEG Data Low-Pass Filtered at 30 Hz

(A and B) The leftside of this figure shows the time frequency representations of power (Panel A) and topographies (B) in the same way as in Figure 2. In comparison with ICA based denoising on individual gamma band filtered data (Figure 2) the alpha band effect is stronger, while the gamma band effect relative to baseline is reduced. The topography of the effect shows

the largest effect on roughly the same electrodes as for the gamma band effect. The effect is however spread out over a larger area. The difference in scale also indicates the topographies over subjects are more variable than for a denoising strategy based on individual gamma band filtered data.

(C–F) The right side of the figure (panels C–F) shows the BOLD-EEG correlations for this approach in the same way as in Figure 3. The top row shows the power effect during visual stimulation relative to baseline. The bottom shows the frequency specific BOLD-power coupling. Compared to denoising with ICA weights estimated on individual gamma band filtered data, a significant positive relation between gamma and BOLD is not observed here (see Figure 3). In accord with this analysis however, negative correlations between BOLD and alpha and beta band power are observed also in this case. The band width of the beta band effect however is smaller here. In accord with this analysis however, negative correlations between BOLD and alpha and beta band power are observed also in this case. The band width of the beta band effect however is smaller here.

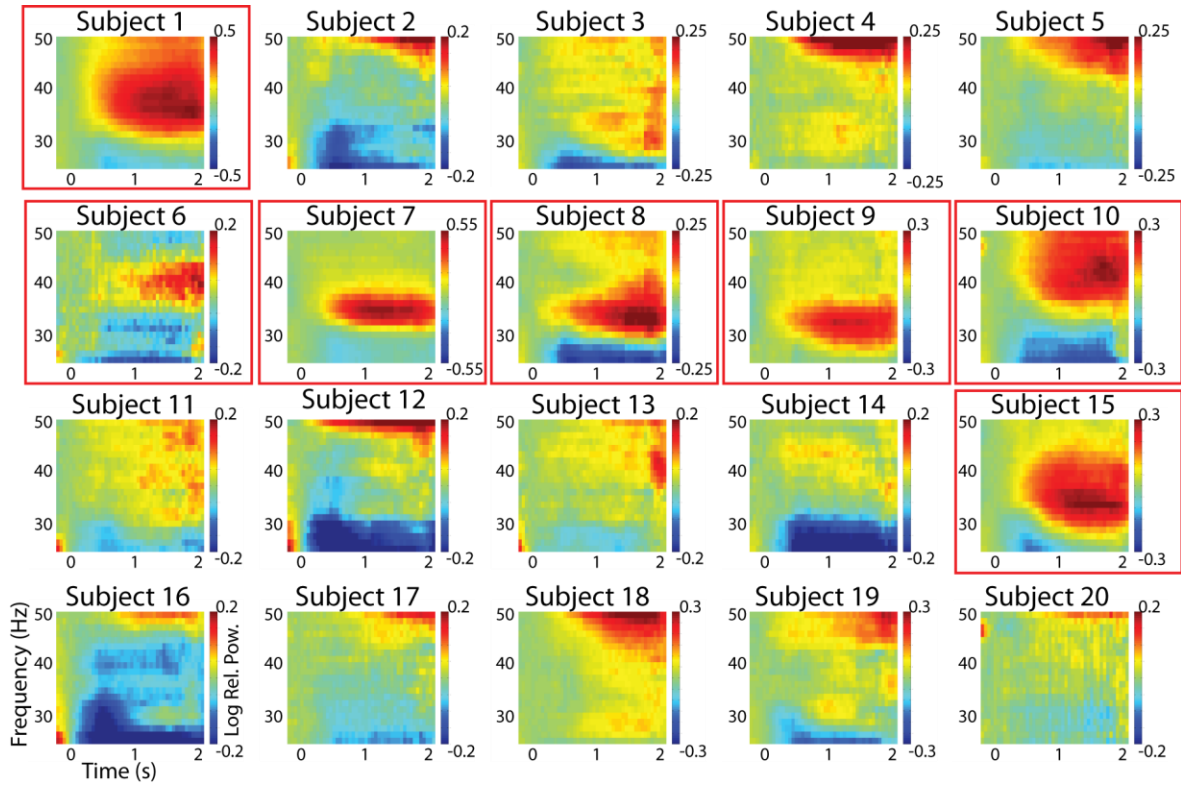


Figure S3, Related to Figure 4. Individual, ICA-Denoised Time-Frequency Analysis of Power of the EEG in the Low Gamma Range for All Subjects

The seven subjects indicated by a red rectangle were included in the analysis focussed on the lower gamma band depicted in Figure 4.